International Journal for Research in Engineering Application & Management (IJREAM)
ISSN : 2454-9150 Vol-04, Issue-07, Oct 2018

Combined Effects of MHD, Convective Inertia Forces and Couple Stresses on the Squeeze Film Characteristics of Parallel Circular plates

B.N Hanumagowda, Professor, REVA University, Bangalore, India.

hanumagowda123@rediffmail.com

Syeda Tasneem Fathima, West Monroe, USA. tasneemhashmi@gmail.com

Salma Jamal, Research Scholar, KNS Institute of Technology, Bangalore, India.

salmajamal.maths@gmail.com

Abstract: **A theoretical study of the combined effects of non-Newtonian couple stresses and convective fluid inertia forces upon the squeeze film characteristics of two parallel circular plates in the presence of externally applied magnetic field is investigated. Based upon the magneto-hydrodynamic flow theory together with the Stokes continuum theory and the averaged inertia principle, a modified Reynolds equation is derived which is solved by using appropriate boundary conditions to obtain squeeze film pressure, load-carrying capacity and squeeze film time. According to the results evaluated, the effects of magnetic field, convective inertia forces and couple stresses provide an increase in the film pressure, the load carrying capacity and the response time. The results are compared with the corresponding non-magnetic inertia less Newtonian lubricant case.**

Keywords —Convective Inertia Forces, Couple Stresses, MHD, Squeeze Film.

I. INTRODUCTION

By the development of modern machine elements, a variety of lubricants have been considered to meet the specific requirements of the bearings which work under severe operating conditions. Since the viscosity varies unexpectedly with temperature, the practice of using liquid metals has achieved extensive interest. They possess high thermal and electrical conductivity. The property of high thermal conductivity reveals that the heat from the source of generation is readily conducted away. In addition, the property of high electrical conductivity implies that hydrodynamic flow behavior can be adjusted by the application of an external magnetic field. Many researchers investigated the effects of MHD on the characteristics of bearings such as slider bearing by Snyder [1], inclined slider bearing and finite step slider bearing by Hughes [2, 3] and parallel plate slider bearing and journal bearing by Kuzma [4, 5]. These studies concluded that the application of magnetic field improves on bearing performance. The study of magnetic field effects on squeeze film lubrication finds applications in hydro-magnetic lubrication of braking devices, hydraulic shock absorbers, astronautical vehicles, slider bearings etc. The MHD squeeze film lubrication has been analyzed by Lin [6, 7] for annular disks and rectangular plates and Lin et al. [8] for curved annular plates. Their study shows that the application of magnetic field enhances the squeeze film pressure, load-carrying capacity and lengthens the response time as compared to the classical non-conducting lubricant case.

In recent years, experimental results have shown clear evidence that a Newtonian viscous lubricant blended with small amount of long-chained additives can improve lubrication properties. According to the experimental contribution to measuring film thickness under boundary lubrication conditions by Spikes [9], a base oil blended with additives can stabilize the behavior of lubricants in elastohydrodynamic contacts and reduce friction and surface damage. The experimental study on the performance of a wet friction clutch by Scott and Suntiwattana [10] revealed that additives have beneficial effects on the friction characteristics and wear of the friction material. Since the classical (Newtonian) continuum theory is incapable of predicting accurate flow behavior of non-Newtonian fluids, many microcontinuum theories describing the peculiar behavior of fluids which contain substructure have been developed [11-13]. Among these theories, the microcontinuum theory generated by Stokes [13] is the simplest theory of fluids which allows for polar effects such as the presence of couple stresses, body couples and non-symmetric tensors. On the basis of this microcontinuum theory of Stokes, a number of investigators have applied the couple stress fluid model to study the lubrication performance of various squeeze film bearings, such as the squeeze film Journal bearings by Lin [14, 15], the parallel stepped squeeze films plates by Kashinath [16] and the squeeze films between circular stepped plates by Naduvinamani and Siddangouda [17]. According to their results, the presence of non-Newtonian couple stresses provides an increase in the load-carrying capacity and the approaching time compared to the traditional case with a Newtonian lubricant.

On the basis of results obtained in the studies of MHD effect and couple stress effect, the researchers are devoted

 DOI : 10.18231/2454-9150.2018.0943

towards the study of bearing performance with the combined effect of MHD and couple stress. The combined effects of couple stress and MHD on bearing characteristics are studied by Biradar and Hanumagowda [18], Conical Bearing and Curved Circular Plates by Hanumagowda et al. [19, 20], different types of finite plates by Fathima et al. [21] and squeeze film bearing by Shalini et al. [22]. The results obtained in these studies showed an increase in pressure, load carrying capacity, squeeze film time and frictional force, co-efficient of friction in case of slider bearing as compared to the classical Newtonian hydrodynamic case. Syed Arishiya et al. [23] have analyzed the Magneto-hydrodynamic couplestress cosine form convex curved plates and shown that the combined effect of couple stresses and external magnetic field provide an increase in the load capacity and the response time as compared to the classical Newtonian hydrodynamic convex curved plates. A comparative study on the combined effects of MHD and couplestress fluid on the performance characteristics of wide slider bearing with an exponential and secant film profile has been done by Fathima et al. [24] and have shown that, the exponential slider has significant load carrying capacity and friction as compared to the secant slider.

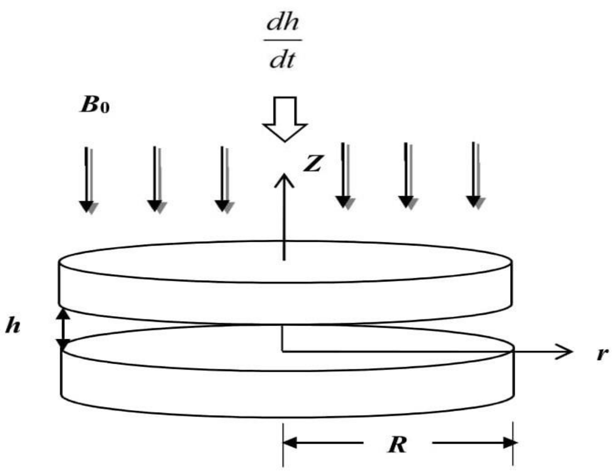

Fig. 1 The squeeze film configuration of parallel circular plates

In all of the above studies, however, the effects of fluid inertia forces are neglected compared to the viscous forces. But in situations where the machine speed is increased or when using low-viscosity and high-density lubricants such as liquid metals, the effects of fluid inertia forces may become relatively significant. Recently there has been extensive investigation on the importance of fluid inertia effects. Lu et al. [25] analyzed the effects of both local inertia and the convective inertia in magneto-hydrodynamic annular squeeze films. It was found that the inertia correction factor in the magneto-hydrodynamic load carrying capacity is more pronounced with large Hartmann numbers. Nabhani and Khlifi [26] have presented numerical solution of fluid inertia effects on inclined slider bearings lubricated by couplestress fluids. They found that the combined effects of fluid inertia forces and couple stresses provide a significant improvement in slider bearing load capacity. Lin et al. [27] showed that the qualitative effects of couple stresses and convective inertia forces on the squeeze film characteristics of two wide parallel plates provide an increase in the film pressure, load capacity and the response time. Dash and Kamila [28] have studied the effect of fluid inertia on the film pressure between two axially oscillating parallel circular plates with a second order fluid as lubricant, whereas Barik et al. [29] extended the analysis by including magnetic field to it. They found that, the visco-elastic lubricant in the presence of magnetic field enhance the efficiency of axially oscillating parallel circular plate type bearings. Further Lin et al. [30] have discussed the effects of couple stresses and convective inertia forces in parallel circular squeeze film plates, but they have restricted their discussion to non-conducting lubricant without the presence of magnetic field. Hence, a further investigation is done in the present study for the squeeze film characteristics of parallel circular plates with couple stresses and inertia forces in the presence of external magnetic field.

In this article, the combined effects of fluid Inertia forces and couple stresses on the squeeze film characteristics between two parallel circular plates with an electrically conducting fluid in the presence of a transverse magnetic field are analyzed. Fluid inertia forces are considered using reduced Navier-Stokes equations for couple stress electrically conducting fluid. The expressions for MHD squeeze film pressure, load-carrying capacity and squeeze film time are obtained and are compared with the classical non-magnetic case by Lin et al. [30].

II. Mathematical Analysis

Figure 1 describes the squeeze film configuration of parallel circular plates of radius R lubricated with an incompressible electrically conducting non-Newtonian couple stress fluid. The lower plate is assumed to be fixed while the upper plate moves normally towards the lower plate with a squeezing velocity $V = -dh/dt$. A uniform transverse magnetic field B_0 is applied perpendicular to the plates.

The following assumptions are made in the present analysis:

1. The couple stress fluid flow in the film region is laminar.
2. The body forces and body couples are negligible except for the Lorentz force
3. The induced magnetic field is small as compared to the externally applied magnetic field.
4. The convective inertia forces due to temporal acceleration are considered.

Under these assumptions, the basic equations of motion for the steady laminar couple stress fluid flow in the film region in the presence of applied magnetic field, retaining the convective inertia terms are given by are given by

$$\rho\left(u\frac{\partial u}{\partial r}+w\frac{\partial u}{\partial z}\right)=\mu\frac{\partial^2 u}{\partial z^2}-\eta\frac{\partial^4 u}{\partial z^4}-\sigma B_0^2 u-\frac{\partial p}{\partial r} \quad (1)$$

$$\frac{\partial p}{\partial z}=0 \quad (2)$$

$$\frac{1}{r}\frac{\partial (ru)}{\partial r}+\frac{\partial w}{\partial z}=0 \quad (3)$$

 DOI : 10.18231/2454-9150.2018.0943

Where u and w are the velocity components in the r and z directions respectively, ρ is the fluid density, μ is the fluid viscosity, η is the material constant responsible for the couple stress fluids, σ is the electrical conductivity of the lubricant and B_0 represents the applied magnetic field.

The relevant boundary conditions for velocity components u and w are the no-slip conditions and the non-couple stress conditions given by:

$$u=0,\ \frac{\partial^2 u}{\partial z^2}=0,\ w=0 \ \text{ at } \ z=0 \tag{4}$$

$$u=0,\ \frac{\partial^2 u}{\partial z^2}=0,\ w=\frac{dh}{dt} \ \text{ at } \ z=h \tag{5}$$

Since the lubricant film is thin, the inertial forces are assumed to remain constant over the film thickness and the convective inertia terms in equation (1) are approximated by the averaged inertia principle as proposed by Mahanti and Ramanaiah [31]:

$$\frac{\rho}{h}\int_0^h\left(u\frac{\partial u}{\partial r}+w\frac{\partial u}{\partial z}\right)dz=-\frac{\partial p}{\partial r}+\mu\frac{\partial^2 u}{\partial z^2}-\eta\frac{\partial^4 u}{\partial z^4}-\sigma B_0^2 u \tag{6}$$

Using the continuity equation and the velocity boundary conditions, the above momentum integral equation can be written as

$$\frac{\rho}{h}\left(\frac{\partial}{\partial r}\int_0^h u^2\,dz+\frac{1}{r}\int_0^h u^2\,dz\right)=-\frac{\partial p}{\partial r}+\mu\frac{\partial^2 u}{\partial z^2}-\eta\frac{\partial^4 u}{\partial z^4}-\sigma B_0^2 u \tag{7}$$

By introducing the modified pressure gradient,

$$f_p=\frac{\partial p}{\partial r}+\frac{\rho}{h}\left\{\frac{\partial}{\partial r}\int_0^h u^2\,dz+\frac{1}{r}\int_0^h u^2\,dz\right\} \tag{8}$$

The momentum equation (7) can be rewritten as

$$\frac{\partial^2 u}{\partial z^2}-\left(\frac{\eta}{\mu}\right)\frac{\partial^4 u}{\partial z^4}-\frac{M^2}{h_0^2}u=\frac{1}{\mu}f_p \tag{9}$$

where $M=B_0h_0\sqrt{\sigma/\mu}$ is the Hartmann number.

Solving equation (9) together with continuity equation (3) and boundary conditions (4) and (5), the radial velocity component is obtained. Three different cases are considered according to the parameter $4l^2M^2/h_0^2$

$$u=\frac{h_0^2 f_p}{\mu M^2}\left[\left(g_1-g_2\right)-1\right] \tag{10}$$

Where

$g_1=g_{11}, g_2=g_{12}$ for $4l^2M^2/h_0^2<1$ (11a)

$g_1=g_{21}, g_2=g_{22}$ for $4l^2M^2/h_0^2=1$ (11b)

$g_1=g_{31}, g_2=g_{32}$ for $4l^2M^2/h_0^2>1$ (11c)

The associated relations in equations (11a), (11b) and (11c) are given in Appendix.

On the other hand the equation of squeezing motion is

$$2\pi r\int_{z=0}^{h}u\,dz=\pi r^2 V \tag{12}$$

Substituting u from (10) into equation (12), the modified pressure gradient function f_p is obtained.

$$f_p=\frac{\mu r}{2f_0(h,l,M)}\frac{dh}{dt} \tag{13}$$

Where

$$f_0(h,l,M)=\begin{cases}\dfrac{h_0^2}{M^2}\left[\dfrac{2l}{\left(A^2-B^2\right)}\left(\dfrac{B^2}{A}tanh\dfrac{Ah}{2l}-\dfrac{A^2}{B}tanh\dfrac{Bh}{2l}\right)+h\right] & for\ \ 4l^2M^2/h_0^2<1\\[2ex] \dfrac{h_0^2}{M^2}\left[\dfrac{h}{2}sech^2\left(\dfrac{h}{2\sqrt{2}l}\right)-3\sqrt{2}l\,tanh\left(\dfrac{h}{2\sqrt{2}l}\right)+h\right] & for\ \ 4l^2M^2/h_0^2=1\\[2ex] \dfrac{h_0^2}{M^2}\left[\dfrac{2lh_0}{M}\left(\dfrac{\left(A\cot\theta-B\right)\sin Bh-\left(B\cot\theta+A\right)\sinh Ah}{\cos Bh+\cosh Ah}\right)+h\right] & for\ \ 4l^2M^2/h_0^2>1\end{cases}$$

Once the modified pressure gradient function has been derived, the squeeze film pressure, the load-carrying capacity and the time-height relationship can be evaluated.

III. SQUEEZE FILM CHARACTERISTICS

Substituting the modified pressure gradient function f_p from equation (13) and the velocity component u from equation (10) into equation (8), one can derive the pressure gradient equation for the squeeze film:

$$\frac{\partial p}{\partial r}=\left[\frac{2\mu hf_0(h,l,M)\left(dh/dt\right)-3\rho f_1(h,l,M)\left(dh/dt\right)^2}{4hf_0^2(h,l,M)}\right]r \tag{14}$$

where $\quad f_1(h,l,M)=\dfrac{h_0^4}{M^4}\left[\left(\xi_1-\xi_2\right)+h\right]$

$\xi_1=\xi_{11}$, $\xi_2=\xi_{12}$ for $4l^2M^2/h_0^2<1$ (15a)

$\xi_1=\xi_{21}$, $\xi_2=\xi_{22}$ for $4l^2M^2/h_0^2=1$ (15b)

$\xi_1=\xi_{31}+\xi_{32}$, $\xi_2=\xi_{33}$ for $4l^2M^2/h_0^2<1$ (15c)

The associated relations in equations (15a), (15b) and (15c) are given in Appendix.

The boundary conditions for the squeeze film pressure are:

$$\frac{dp}{dr}=0 \ \text{ at } \ r=0 \tag{16}$$

$$p=0 \ \text{ at } \ r=R \tag{17}$$

Integrating the pressure gradient equation (14) with respect to r with the above conditions gives the film pressure in non-dimensional form as,

$$p^*=\left[\frac{2h^* f_0\left(h^*,l^*,M\right)+3\,Re\,f_1\left(h^*,l^*,M\right)}{8h^* f_0^2\left(h^*,l^*,M\right)}\right]\left(1-r^{*2}\right) \tag{18}$$

The dimensionless variables and parameters in the above equation are defined by

$$r^*=\frac{r}{R},\ h^*=\frac{h}{h_0},\ l^*=\frac{l}{h_0},\ \mathrm{Re}=\frac{\rho h_0\left(-dh/dt\right)}{\mu} \tag{19a}$$

$$p^*=\frac{ph_0^3}{\mu R^2\left(-dh/dt\right)},\ f_0\left(h^*,l^*,M\right)=\frac{f_0(h,l,M)}{h_0^3} \tag{19b}$$

$$f_1\left(h^*,l^*,M\right)=\frac{f_1(h,l,M)}{h_0^5} \tag{19c}$$

DOI : 10.18231/2454-9150.2018.0943

where

$$f_0\left(h^*,l^*,M\right)=\begin{cases}\dfrac{1}{M^2}\left[\dfrac{2l^*}{\left(A_1^{*2}-B_1^{*2}\right)}\left(\dfrac{B_1^{*2}}{A_1^*}tanh\dfrac{A_1^*h^*}{2l^*}-\dfrac{A_1^{*2}}{B_1^*}tanh\dfrac{B_1^*h^*}{2l^*}\right)+h^*\right] & for \quad 4l^2M^2/h_0^2<1\\ \dfrac{1}{M^2}\left[\dfrac{h^*}{2}sech^2\left(\dfrac{h^*}{2\sqrt{2}l^*}\right)-3\sqrt{2}l^*\,tanh\left(\dfrac{h^*}{2\sqrt{2}l^*}\right)+h^*\right] & for \quad 4l^2M^2/h_0^2=1\\ \dfrac{1}{M^2}\left[\dfrac{2l^*}{M}\left(\dfrac{\left(A_2^*\cot\theta^*-B_2^*\right)\sin B_2^*h^*-\left(B_2^*\cot\theta^*+A_2^*\right)\sinh A_2^*h^*}{\cos B_2^*h^*+\cosh A_2^*h^*}\right)+h^*\right] & for \quad 4l^2M^2/h_0^2>1\end{cases}$$

$$A_1^*=\left(\frac{1+\left(1-4l^{*2}M^2\right)^{1/2}}{2}\right)^{1/2},\quad B_1^*=\left(\frac{1-\left(1-4l^{*2}M^2\right)^{1/2}}{2}\right)^{1/2}$$

$$A_2^*=\sqrt{M/l^*}\,cos\left(\theta^*/2\right),\ B_2^*=\sqrt{M/l^*}\,sin\left(\theta^*/2\right),$$

$$\theta^*=tan^{-1}\left(\sqrt{4l^{*2}M^2-1}\right)$$

$$f_1\left(h^*,l^*,M\right)=\frac{1}{M^4}\left[\left(\xi_1^*-\xi_2^*\right)+h\right]$$

$$\xi_1^*=\xi_{11}^*,\qquad \xi_2^*=\xi_{12}^*\quad for\quad 4l^2M^2/h_0^2<1 \qquad (20a)$$

$$\xi_1^*=\xi_{21}^*,\qquad \xi_2^*=\xi_{22}^*\quad for\quad 4l^2M^2/h_0^2=1 \qquad (20b)$$

$$\xi_1^*=\xi_{31}^*+\xi_{32}^*,\qquad \xi_2^*=\xi_{33}^*\quad for\quad 4l^2M^2/h_0^2<1 \qquad (20c)$$

The associated relations in equations (20a), (20b) and (20c) are given in Appendix.

The load-carrying capacity is now obtained by integrating the film pressure acting upon the upper plate.

$$W=2\pi\int_{r=0}^{r=R} pr\,dr \qquad (21)$$

After performing the integration, the non-dimensional load carrying capacity is obtained,

$$W^*=\frac{Wh_0^3}{\mu R^4\left(-dh/dt\right)}=\frac{2\pi h^*f_0\left(h^*,l^*,M\right)+3\pi\,Re\,f_1\left(h^*,l^*,M\right)}{16h^*f_0^2\left(h^*,l^*,M\right)} \qquad (22)$$

To obtain the approaching time, a non-dimensional definition t^* is introduced:

$$t^*=\frac{Wh_0^2}{\mu R^4}t \qquad (23)$$

The time-height relationship is then obtained from equation (22) as

$$\frac{dh^*}{dt^*}=-\frac{16h^*f_0^2\left(h^*,l^*,M\right)}{2\pi h^*f_0\left(h^*,l^*,M\right)+3\pi\,Re\,f_1\left(h^*,l^*,M\right)} \qquad (24)$$

Applying the initial condition for the non-dimensional film height (i.e., $h^*=1\ at\ t^*=0$), the non-dimensional approaching time can be derived by integrating the differential equation (24):

$$t^*=-\int_1^{h_1^*}\frac{2\pi h^*f_0\left(h^*,l^*,M\right)+3\pi\,Re\,f_1\left(h^*,l^*,M\right)}{16h^*f_0^2\left(h^*,l^*,M\right)}dh^* \qquad (25)$$

As $M\rightarrow 0$, equations of p^*, W^* and t^* reduces to corresponding non-magnetic case [30].

IV. Results And Discussions

In order to study the squeeze film characteristics on the MHD parallel circular plates with convective inertia forces and non-Newtonian fluid blended with lubricant additives, the numerical computations are performed for various non-dimensional parameters viz., couple stress parameter l^*, Hartmann number M and Reynolds number Re. l^* signifies the couple stress effect resulting from the lubricant blended with various additives, M signifies the effect of magnetic field and is applied transversely and Re signifies the effect of convective inertia resulting from temporal acceleration of the fluid.

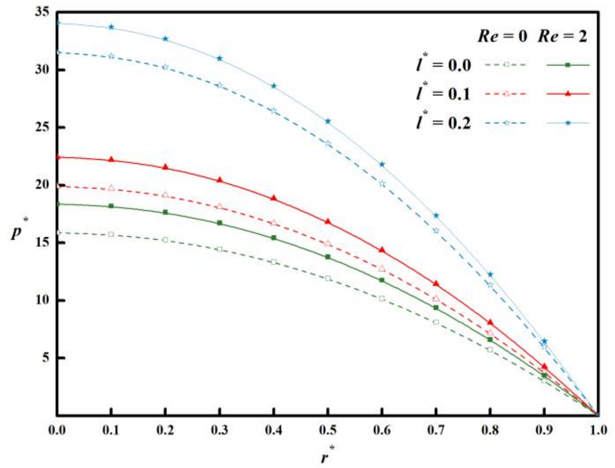

Fig. 2 Variation of dimensionless pressure p^* with r^* for different values of l^* and Re at $h^*=0.6$ and $M=2$.

A. *Squeeze film pressure*

Figure 2 shows the variation of non-dimensional film pressure p^* with dimensionless radius r^* for different values of couple stress parameter l^* under both non-inertia ($Re=0$) and inertia ($Re=2$) cases. It is observed that the effects of couple stresses ($l^*=0.1,0.2$) results in a higher film pressure as compared to the Newtonian lubricant case ($l^*=0$). Also the convective inertia forces provide a further increase in pressure as compared to the non-inertia case.

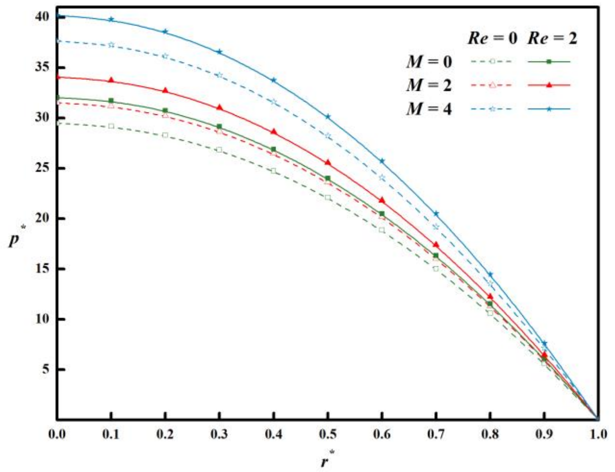

Fig. 3 Variation of dimensionless pressure p^* with r^* for different values of M and Re at $h^*=0.6$ and $l^*=0.2$.

 DOI : 10.18231/2454-9150.2018.0943

The variation of non-dimensional film pressure p^* with r^* for various values of Hartmann number M and Reynolds number Re is depicted in Figure 3. It is clear that the film pressure increases when the magnetic field is applied ($M = 2, 4$) under both non-inertia as well as inertia case. On the whole the combined effect of magnetic field and convective inertia is to increase the film pressure considerably.

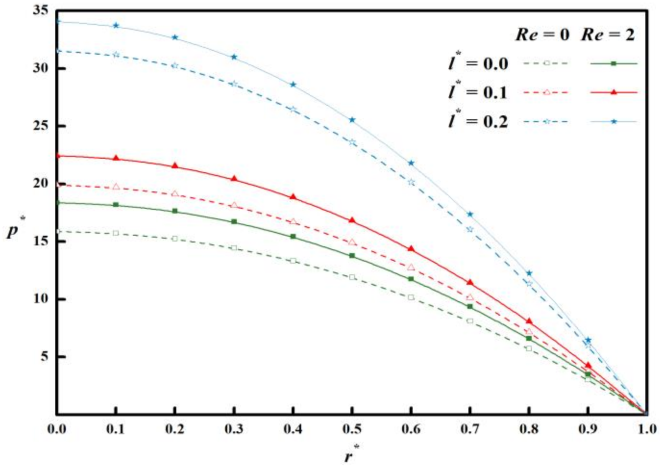

Fig. 4 Variation of dimensionless load W^* with h^* for different values of l^* and Re at $M = 2$.

B. *Load-carrying capacity*

Figure 4 displays the non-dimensional load carrying capacity W^* with dimensionless film height h^* for different values of couple stress parameter l^* with Reynolds number $Re = 0$ and $Re = 2$. Since the couple stress effects yields a higher film pressure, the integrated load carrying capacity is similarly affected. Comparing with the Newtonian lubricant case ($l^* = 0$), the effect of couple stresses increase the load carrying capacity; and larger increments are obtained by the use of convective inertia force. Figure 5 presents the variation of W^* as a function of h^* for various values of Hartmann number M with $Re = 0, 2$. Since the effect of magnetic field yields a higher pressure, the integration of the various pressure distribution curves results in the functional dependence of the load carrying capacity upon the Hartmann number. Compared with the non-conducting lubricant case ($M = 0$), an increase in the load carrying capacity is obtained when the magnetic field is applied. As the convective inertia is included, a higher load carrying capacity is obtained for the squeeze film motion.

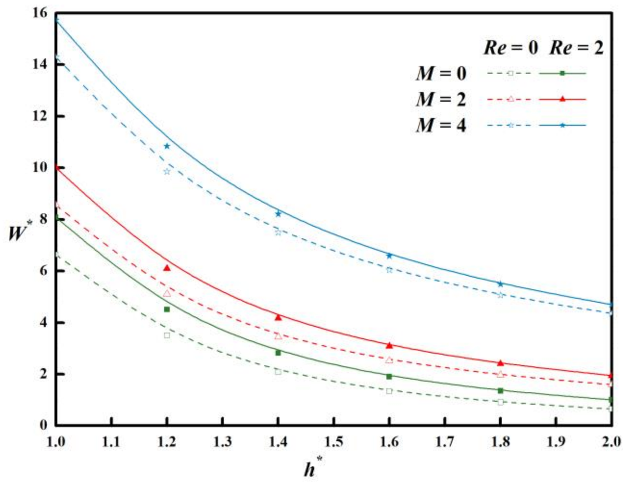

Fig. 5 Variation of dimensionless load W^* with h^* for different values of M and Re at $l^* = 0.2$.

C. *Squeeze film time*

Figure 6 describes the variation of non-dimensional time of approach t^* as a function of h_1^* for different values of l^* with $Re = 0$ and $Re = 2$. It is observed that for both non-inertia and inertia case, the effect of couple stress parameter is to delay the time of approach. As the couple stress fluid offers more resistance to the moving fluid, a larger amount of fluid would remain in the film region and offers more delayed dimensionless time compared to Newtonian cases. The effect of convective fluid inertia provides a further increase in the response time. Figure 7 represents the variation of t^* with h_1^* for various values of M under the non-inertia and inertia cases. The effect of magnetic field is to increase the dimensionless time as a consequence of the resistive Lorentz force. Moreover, the increase in the Reynolds number results in further increase of the dimensionless time, as the inertia forces offers more resistance to the fluid flow, a larger amount of fluid would remain in the film region and offers more delayed dimensionless time compared to non-inertia case.

V. CONCLUSION

The effects of MHD and convective inertia forces on the squeeze film characteristics of parallel circular plates lubricated with couple stress fluid are presented. The modified Reynolds equation is derived using Stokes micro-continuum theory together with the magneto-hydrodynamic flow theory and the principle of averaged inertia. From the results obtained, the following conclusions are drawn.

- The effect of magnetic field increases the build-up pressure between the parallel circular plates.
- The couple stress fluids contain microstructure additives and are sensitive to the applied magnetic field. As a result there is an enhancement in the load carrying capacity and the response time.
- An increase in the film pressure, load carrying capacity and squeeze film time is predicted as the convective inertia is considered.
- Comparing with the non-conducting Newtonian non-inertia case, the combined effects of magnetic field, couple stresses and convective inertia forces increases the

 DOI : 10.18231/2454-9150.2018.0943

film pressure and load carrying capacity considerably and also lengthens the squeeze film time.

- The quantitative effects of magnetic field, couple stresses and convective inertia forces on the squeeze film characteristics are more pronounced with a smaller squeeze film height and a larger couple stress parameter, Hartmann number and Reynolds number.
- As $M \rightarrow 0$, the present analysis reduces to the non-magnetic case by Lin et al. [30].

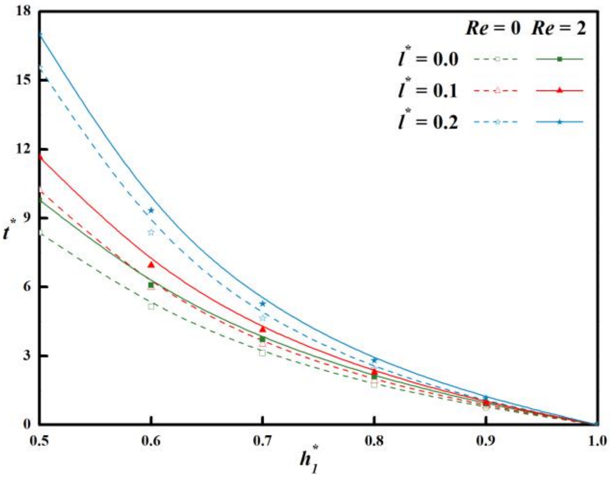

Fig. 6 Variation of dimensionless squeeze film time t^* with h_1^* for different values of l^* and Re at $M = 2$.

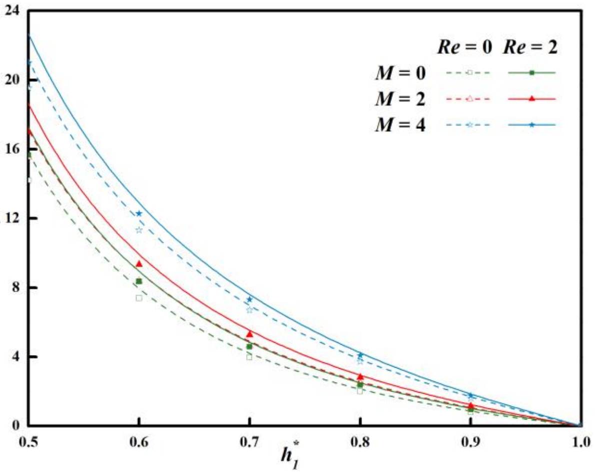

Fig. 7 Variation of dimensionless squeeze film time t^* with h_1^* for different values of M and Re at $l^* = 0.2$.

APPENDIX

$$g_{11} = \frac{A_1^2}{A_1^2 - B_1^2}\frac{\cosh\{B_1(2z-h)/2l\}}{\cosh(B_1 h/2l)} \tag{a1}$$

$$g_{12} = \frac{B_1^2}{A_1^2 - B_1^2}\frac{\cosh\{A_1(2z-h)/2l\}}{\cosh(A_1 h/2l)} \tag{a2}$$

$$A_1 = \left[\frac{1+\left\{1-\left(4l^2M^2/h_0^2\right)\right\}^{1/2}}{2}\right]^{1/2} \tag{a3}$$

$$B_1 = \left[\frac{1-\left\{1-\left(4l^2M^2/h_0^2\right)\right\}^{1/2}}{2}\right]^{1/2} \tag{a4}$$

$$g_{21} = \frac{2\cosh\{(z-h)/\sqrt{2}l\} + 2\cosh(z/\sqrt{2}l)}{2\{\cosh(h/\sqrt{2}l)+1\}} \tag{b1}$$

$$g_{22} = \frac{(z/\sqrt{2}l)\sinh\{(z-h)/\sqrt{2}l\} + \{(z-h)/\sqrt{2}l\}\sinh(z/\sqrt{2}l)}{2\{\cosh(h/\sqrt{2}l)+1\}} \tag{b2}$$

$$g_{31} = \frac{\cos B_2 z\cosh A_2(z-h) + \cosh A_2 z\cos B_2(z-h)}{\cosh A_2 h + \cos B_2 h} \tag{c1}$$

$$g_{32} = \frac{\cot\theta\{\sinh A_2 z\sin B_2(z-h) + \sin B_2 z\sinh A_2(z-h)\}}{\cosh A_2 h + \cos B_2 h} \tag{c2}$$

$$A_2 = \sqrt{M/lh_0}\cos(\theta/2) \tag{c3}$$

$$B_2 = \sqrt{M/lh_0}\sin(\theta/2) \tag{c4}$$

$$\theta = \tan^{-1}\left(\sqrt{4l^2M^2/h_0^2 - 1}\right) \tag{c5}$$

$$\xi_{11} = \frac{h}{2(A^2-B^2)^2}\left\{B^4\operatorname{sech}^2\frac{Ah}{2l} + A^4\operatorname{sech}^2\frac{Bh}{2l}\right\} \tag{d1}$$

$$\xi_{12} = \frac{l}{(A^2-B^2)^3}\left\{\frac{B^4(7A^2-3B^2)}{A}\tanh\frac{Ah}{2l} - \frac{A^4(7B^2-3A^2)}{B}\tanh\frac{Bh}{2l}\right\} \tag{d2}$$

$$\xi_{21} = \left(\frac{19h}{16} + \frac{h^3}{96l^2}\right)\operatorname{sech}^2\left(\frac{h}{2\sqrt{2}l}\right) + \frac{h^2}{4\sqrt{2}l}\operatorname{sech}^2\left(\frac{h}{2\sqrt{2}l}\right)\tanh\left(\frac{h}{2\sqrt{2}l}\right) \tag{d3}$$

$$\xi_{22} = \frac{h^3}{64l^2}\operatorname{sech}^4\left(\frac{h}{2\sqrt{2}l}\right) + \frac{35l}{4\sqrt{2}}\tanh\left(\frac{h}{2\sqrt{2}l}\right) \tag{d4}$$

$$\xi_{31} = \frac{lh_0}{M_0^2}\left\{\frac{\left[M_0 - lh_0(A+B\cot\theta)(7A-B\cot\theta)\right]B\sinh Ah}{\sin\theta(\cosh Ah+\cos Bh)}\right\} \tag{d5}$$

$$\xi_{32} = \frac{lh_0}{M_0^2}\left\{\frac{\left[M_0 - lh_0(B-A\cot\theta)(7B+A\cot\theta)\right]A\sin Bh}{\sin\theta(\cosh Ah+\cos Bh)}\right\} \tag{d6}$$

$$\xi_{33} = \frac{\left[(\cot^2\theta-1)(1+\cosh Ah\cos Bh) - 2\cot\theta\sinh Ah\sin Bh\right]h}{2(\cosh Ah+\cos Bh)^2} \tag{d7}$$

$$\xi_{11}^* = \frac{h^*}{2\left(A^{*2}-B^{*2}\right)^2}\left\{B^{*4}\sec h^2\frac{A^*h^*}{2l^*} + A^{*4}\sec h^2\frac{B^*h^*}{2l^*}\right\} \tag{e1}$$

$$\xi_{12}^* = \frac{l^*}{\left(A^{*2}-B^{*2}\right)^3}\left\{\frac{B^{*4}\left(7A^{*2}-3B^{*2}\right)}{A^*}\tanh\frac{A^*h^*}{2l^*} - \frac{A^{*4}\left(7B^{*2}-3A^{*2}\right)}{B^*}\tanh\frac{B^*h^*}{2l^*}\right\}$$

 DOI : 10.18231/2454-9150.2018.0943

ISSN : 2454-9150 Vol-04, Issue-07, Oct 2018

(e2)

$$\xi_{21}^{*}=\left(\frac{19h^{*}}{16}+\frac{h^{*3}}{96l^{*2}}\right)sech^{2}\left(\frac{h^{*}}{2\sqrt{2}l^{*}}\right)+\frac{h^{*2}}{4\sqrt{2}l^{*}}sech^{2}\left(\frac{h^{*}}{2\sqrt{2}l^{*}}\right)tanh\left(\frac{h^{*}}{2\sqrt{2}l^{*}}\right)$$

(e3)

$$\xi_{22}^{*}=\frac{h^{*3}}{64l^{*2}}sech^{4}\left(\frac{h^{*}}{2\sqrt{2}l^{*}}\right)+\frac{35l^{*}}{4\sqrt{2}}tanh\left(\frac{h^{*}}{2\sqrt{2}l^{*}}\right)$$

(e4)

$$\xi_{31}^{*}=\frac{l^{*}}{M_{0}^{2}}\left\{\frac{\left[M_{0}-l^{*}\left(A^{*}+B^{*}\cot\theta^{*}\right)\left(7A^{*}-B^{*}\cot\theta^{*}\right)\right]B^{*}\sinh A^{*}h^{*}}{\sin\theta^{*}\left(\cosh A^{*}h^{*}+\cos B^{*}h^{*}\right)}\right\}$$

(e5)

$$\xi_{32}^{*}=\frac{l^{*}}{M_{0}^{2}}\left\{\frac{\left[M_{0}-l^{*}\left(B^{*}-A^{*}\cot\theta^{*}\right)\left(7B^{*}+A^{*}\cot\theta^{*}\right)\right]A^{*}\sin B^{*}h^{*}}{\sin\theta^{*}\left(\cosh A^{*}h^{*}+\cos B^{*}h^{*}\right)}\right\}$$

(e6)

$$\xi_{33}^{*}=\frac{\left[\left(\cot^{2}\theta^{*}-1\right)\left(1+\cosh A^{*}h^{*}\cos B^{*}h^{*}\right)-2\cot\theta^{*}\sinh A^{*}h^{*}\sin B^{*}h^{*}\right]h^{*}}{2\left(\cosh A^{*}h^{*}+\cos B^{*}h^{*}\right)^{2}}$$

(e7)

NOMENCLATURE

h film thickness
h^* non-dimensional film thickness (h/h_0)
h_0 initial film thickness
h_1 film thickness after time Δt
h_1^* non-dimensional film thickness after time Δt
l couplestress parameter $(\eta/\mu)^{1/2}$
l^* non-dimensional couplestress parameter (l/h_0)
Re Reynolds number $(\rho h_0 V/\mu)$
p pressure in the film region
p^* non-dimensional fluid film pressure $(ph_0^3/\mu R^2 V)$
W load capacity of the squeeze film
W^* non-dimensional load capacity $(Wh_0^3/\mu R^4 V)$
t time of approach of the upper plate
t^* non-dimensional time $(Wh_0^2 t/\mu R^4)$

REFERENCES

[1] W. T. Snyder, "The magnetohydrodynamic slider bearing", Journal of Fluids Engineering, vol. 84, no. 1, pp. 197-202, 1962.
[2] W. F. Hughes, "The magnetohydrodynamic inclined slider bearing with a transverse magnetic field", Wear, vol. 6, no. 4, pp. 315-324, 1963.
[3] W. F. Hughes, "The magnetohydrodynamic finite step slider bearing", Journal of Basic Engineering, vol. 85, no. 1, pp. 129-136, 1963.
[4] D. C. Kuzma, "The magnetohydrodynamic parallel plate slider bearing", ASME Journal of Basic Enginnering, vol. 87, no. 3, pp. 778-780, 1964.
[5] D. C. Kuzma, "The magnetohydrodynamic journal bearing", Journal of Basic Engineering, vol. 85, no. 3, pp. 424-427, 1963.
[6] J. R. Lin, "Magneto-hydrodynamic squeeze film characteristics between annular disks", Industrial Lubrication and Tribology, vol. 53, no. 2, pp. 66-71, 2001.
[7] J. R. Lin, "Magneto-hydrodynamic squeeze film characteristics for finite rectangular plates", Industrial Lubrication and Tribology, vol. 55, no. 2, pp. 84-89, 2003.
[8] J. R. Lin, R. F. Lu, W. H. Liao, "Analysis of magneto-hydrodynamic squeeze film characteristics between curved annular plates", Industrial Lubrication and Tribology, vol. 56, no. 5, pp. 300-305, 2004.
[9] H. A. Spikes, "The behaviour of lubricants in contacts: current understanding and future possibilities", J. Proc. Instn. Mech. Engrs, vol. 208, no. 1, pp. 3–15, 1994.
[10] W. Scott, P. Suntiwattana, "Effect of oil additives on the performance of a wet friction clutch material", Wear, vol. 181-183, pp. 850–855, 1995.
[11] T. Ariman, M. A. Turk, N. D. Sylvester, "Micro continuum fluid mechanics-a review", International journal of Engineering science, vol. 11, no. 8, pp. 905-930, 1973.
[12] T. Ariman, M. A. Turk, N. D. Sylvester, "Application of micro continuum fluid mechanics", International journal of Engineering science, vol. 12, no. 4, pp. 273-293, 1974.
[13] V. K. Stokes, "Couple stresses in fluids", Physics of Fluids, vol. 9, no. 9, pp. 1709-1715, 1966.
[14] J. R. Lin, "Squeeze film characteristics of long partial journal bearings lubricated with couple stress fluids", Tribology International, vol. 30, no. 1, pp. 53-58, 1997.
[15] J. R. Lin, "Squeeze film characteristics of finite journal bearings: couple stress fluid model", Tribology International, vol. 31, no. 4, pp. 201-207, 1998.
[16] Biradar Kashinath, "Squeeze Film Lubrication between Parallel Stepped Plates with Couplestress Fluids", vol. 3, no. 2, pp. 65-69, 2012.
[17] N. B. Naduvinamani, A. Siddangouda, "Squeeze film lubrication between circular stepped plates of couple stress fluids", Braz Soc Mech Sci Eng, vol. XXXI, no. 1, pp. 21–26, 2009.
[18] Biradar Kasinath, B. N. Hanumagowda, "MHD Effects on Composite Slider Bearing Lubricated with Couple-stress Fluids", Int J. Math trends and Tech, vol. 5, pp. 27-49, 2014.
[19] B. N. Hanumagowda, Swapna Nair, M. Vishu Kumar, "Effect of MHD and Couple Stress on Conical Bearing", Int. J. Pure and Applied Math., vol. 113, no. 6, pp. 316-324, 2017.
[20] B. N. Hanumagowda, A. Salma, B. T. Raju, C. S. Nagarajappa, "The Magneto-hydrodynamic Lubrication of Curved Circular Plates With Couple Stress Fluid", Int. J. Pure and Applied Math., vol. 113, no. 6, pp. 307-315, 2017.
[21] Syeda Tasneem Fathima, N. B. Naduvinamani, B. N. Hanumagowda, J. Santhosh Kumar, "Modified Reynolds Equation for Different Types of Finite Plates with the Combined Effect of MHD and Couple Stresses", Tribology Transactions, vol. 58, pp. 660-667, 2015.
[22] Shalini M Patil, P. A. Dinesh, C. V. Vinay, "Combined effects of couple stress and MHD on squeeze film lubrication between two parallel plates", Int. J.

 DOI : 10.18231/2454-9150.2018.0943

Mathematical Archive, vol. 4, no. 12, pp. 165-171, 2013.
[23] Syed Arishiya Naseem Fatima, T. Biradar, S. T. Fathima, B. N. Hanumagowda, “Magneto-hydrodynamic couplestress cosine form convex curved plates”, Int. J. Mathematical Archive, vol. 7, no. 7, pp. 44-52, 2016.
[24] Syeda Tasneem Fathima, N. B. Naduvinamani, C. K. Sreekala, B. N. Hanumagowda, “The effect of MHD and couplestress fluid on the performance characteristics of wide slider bearing with an exponential and secant film profile-A comparative study”, Int. J. Mathematical Archive, vol. 7, no. 5, pp. 141-150, 2016.
[25] R. F. Lu, R. D. Chien, J. R. Lin, “Effects of fluid inertia in magneto-hydrodynamic annular squeeze films”, Tribology International, vol. 39, pp. 221-226, 2006.
[26] Mohamed Nabhani, Mohamed El Khilfi, “Inertia Effects on Inclined Slider Bearings Lubricated by a Couple Stress Fluid”, Tribology Transactions, vol. 57, pp. 515-523, 2014.
[27] J. R. Lin, C. R. Hung, R. F. Lu, “Averaged Inertia principle for non-Newtonian squeeze films in wide parallel plates: Couple stress fluid”, J. Marine Science and Technology, vol. 14, no. 4, pp. 218-224, 2006.
[28] G. C. Dash, R. K. Kamila, “The effect of fluid inertia on the film pressure between two axially oscillating parallel circular plates”, AMSE Journals, Modelling B, Simulation & Control, vol. 21, no. 1, pp. 55-62, 1989.
[29] M. Barik, G. C. Dash, R. N. Barik, “The Effect of Magnetic Field and Fluid Inertia on the Film Pressure between Two Axially Oscillating Parallel Circular Plates with a Second Order Fluid as Lubricant”, ASME, vol. 84, no. 2, pp. 39-51, 2015.
[30] J. R. Lin, R. F. Lu, W. H. Liao, C. C. Kuo, “Effects of couple stresses and convective inertia forces in parallel circular squeeze-film plates”, Industrial Lubrication and Tribology, vol. 56, no. 6, pp. 318-323, 2004.
[31] A. C. Mahanti, G. R. Ramanaiah, “Inertia effect of micropolar fluid squeeze film bearings and thrust bearings”, Wear, vol. 39, pp. 227–238, 1976.

 DOI : 10.18231/2454-9150.2018.0943